

Article

The Role of Cations and Anions in the Formation of Crystallization Oligomers in Protein Solutions as Revealed by Combination of Small-Angle X-ray Scattering and Molecular Dynamics

Margarita A. Marchenkova ^{1,*}, Petr V. Konarev ¹ , Yuliya V. Kordonskaya ², Kseniia B. Ilina ¹, Yury V. Pisarevsky ^{1,2}, Alexander V. Soldatov ³ , Vladimir I. Timofeev ¹ and Mikhail V. Kovalchuk ^{1,2}

¹ A.V. Shubnikov Institute of Crystallography, Federal Scientific Research Centre “Crystallography and Photonics”, Russian Academy of Sciences, 59, Leninskii Prospect, Moscow 119333, Russia; peter_konarev@mail.ru (P.V.K.); xenium-xyz@mail.ru (K.B.I.); yupisarev@yandex.ru (Y.V.P.); tostars@mail.ru (V.I.T.); koval@ns.crys.ras.ru (M.V.K.)

² National Research Centre “Kurchatov Institute”, 1, Akademika Kurchatova pl., Moscow 123182, Russia; yukord@mail.ru

³ The Smart Materials Research Institute, Southern Federal University, 178/124, Andreyka Sladkova Street, Rostov on Don 344090, Russia; soldatov@sfned.ru

* Correspondence: marchenkova@crys.ras.ru



Citation: Marchenkova, M.A.; Konarev, P.V.; Kordonskaya, Y.V.; Ilina, K.B.; Pisarevsky, Y.V.; Soldatov, A.V.; Timofeev, V.I.; Kovalchuk, M.V. The Role of Cations and Anions in the Formation of Crystallization Oligomers in Protein Solutions as Revealed by Combination of Small-Angle X-ray Scattering and Molecular Dynamics. *Crystals* **2022**, *12*, 751. <https://doi.org/10.3390/cryst12060751>

Academic Editor: Abel Moreno

Received: 19 April 2022

Accepted: 22 May 2022

Published: 24 May 2022

Publisher’s Note: MDPI stays neutral with regard to jurisdictional claims in published maps and institutional affiliations.



Copyright: © 2022 by the authors. Licensee MDPI, Basel, Switzerland. This article is an open access article distributed under the terms and conditions of the Creative Commons Attribution (CC BY) license (<https://creativecommons.org/licenses/by/4.0/>).

Abstract: As is known from molecular dynamics simulation, lysozyme oligomers in crystallization solutions are most stable when taking into account as many precipitant ions as possible embedded in the corresponding crystal structure. Therefore, the number of precipitant ions associated with crystallographic oligomer models can play a role during the modeling of small-angle X-ray scattering (SAXS) data. This hypothesis has been tested in the present work. As a result, it turned out that the best fit quality to the experimental SAXS data is reached when using oligomers without precipitant ions at all or with embedded chlorine ions. Molecular dynamics (MD) simulation shows that the stability of crystallization oligomers depends on the consideration of anions and cations in oligomer structure. Thus, it is chlorine ions which stabilize dimer and octamers in lysozyme crystallization solution. As SAXS is more sensitive to the role of cations and MD shows the role of anions which are “light” for X-rays, it has been shown that precipitant cations most likely do not bind to monomers, but to already-formed oligomers.

Keywords: protein crystallography; small-angle X-ray scattering; molecular dynamics simulation; precipitant ions; lysozyme oligomers; protein crystallization

1. Introduction

The problem of the relative efficiency of various ions in the lysozyme crystallization has been considered for many years [1,2]. Hofmeister in reference [3] showed that the solubility of lysozyme mainly depends on anions and only slightly on cations. In reference [2], it was also found that according to the order of effectiveness of salts with different anions (pTs^- , SCN^- , NO_3^- , Cl^- , and $H_2PO_4^-$) decreasing the lysozyme solubility, there are differences in their ability to switch protein interactions to attractive ones, while the cations (Li^+ , Na^+ , K^+ , Cs^+ , and NH_4^+) did not have a noticeable effect on this.

With the predominance of repulsive forces between proteins, they tend to remain as far apart as possible, while the added precipitating agent, which promotes crystallization, leads to the mutual attraction of protein molecules [2], because of which we assume the formation of oligomers occurs. Switching the type of interaction of protein molecules can take place due to changes arising both near the surface of the lysozyme (for example, due

to screening of surface charges by precipitant ions) or in a bulk solvent (or due to the both factors simultaneously) [2].

In recent works [4–6], it has been found that before the crystallization of lysozyme, its oligomers are formed in the solution, playing the role of precursor clusters in the formation of the protein crystal.

In reference [7], it was determined that under conditions with different precipitants, the number of cations and anions bound to the lysozyme molecule is different (Figure 1): in the structure with PDB ID: 4WLD, only one sodium ion is taken into account, and in the structures with PDB IDs: 6QWY, 6QWW, 6QWX, 6QWZ, and 6QX0, the positions of chlorine ions and additional metal ions bound to the lysozyme molecule were determined in the lattice. In order to assess the stability of such oligomers and study the behavior of atoms and bonds in their structure, it was proposed to use the molecular dynamics method [8,9]. The work [9] shows that with rising temperature, RMSF of lysozyme dimers and octamers increases (i.e., oligomers stability declines) in a regular way only when simulations have been performed for models accounting for all precipitant ions associated with the protein. Therefore, the correspondence of molecular dynamics results to the temperature investigations of tetragonal lysozyme crystallization solutions by SAXS is achieved only by taking into account all precipitant ions in calculations. In addition, dimers remain more stable with precipitant ions (at least anions) embedded in the protein than without them [10]. However, a model with only one sodium ion was used to process the same data [4]. This paper analyzes the influence of the crystallographic models of lysozyme precursor clusters with different occupancy of the precipitant ions on their fit quality to experimental SAXS data.

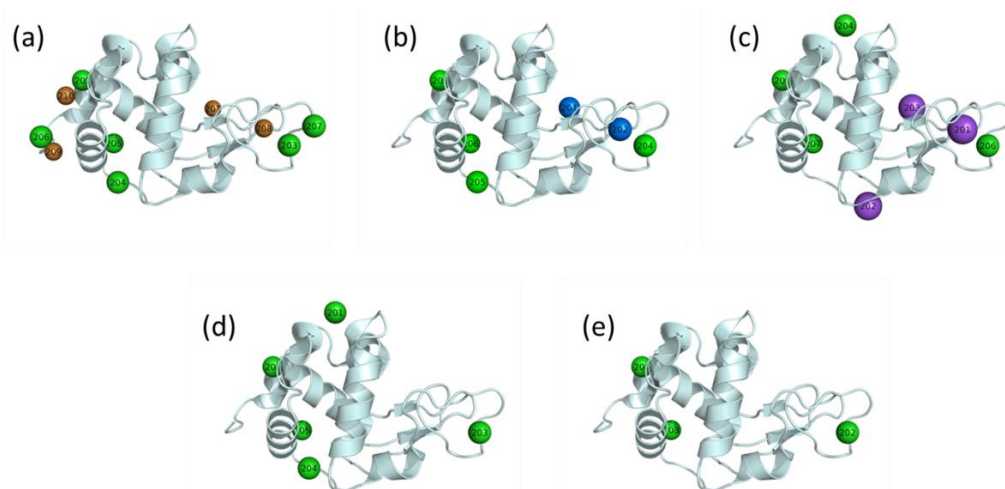


Figure 1. The location of metal (red sphere) and chloride (green sphere) ions associated with the lysozyme molecule in Cu-(a), Ni-(b), Na-(c), K-(d), and Li-crystals (e).

2. Materials and Methods

SAXS data analysis. The samples were fabricated using hen’s egg lysozyme (Sigma-Aldrich, Burlington, MA, USA, CAS no. 12650-88-3). The mother liquors were prepared using the following inorganic salts: LiCl (technical specifications 6-09-3751-83, Laverna Stroiinzhiniring, Saratov, Russia), NaCl (CAS no. 7647-14-5, Helicon, Moscow, Russia), KCl (CAS no. 7447-40-7, abcr GmbH), NiCl₂ (CAS no. 7791-20-0, Alta Aesar, Ward Hill, MA, USA), and CuCl₂ (CAS no. 7447-39-4, Acros Organics, Geel, Belgium). All solutions were prepared using Millipore ultrapure water (water resistance 18 MΩ cm). The protein and salts were dissolved in 0.2 M sodium acetate buffer (pH 4.5). The salt solutions were filtered using Millex membrane syringe filters with a pore size of 0.22 μm; the protein solution was centrifuged with a rate of 10,000 rpm for 10 min. The initial concentration in the protein mother liquor was 80 mg/mL, and the initial concentrations of all salts in the mother liquors were 0.8 M.

Before carrying out SAXS measurements, the lysozyme and salt mother liquors were poured together and mixed in equal volumes. The series of experiments were carried out on the P12 (EMBL, Hamburg, Germany) small-angle scattering beamline. The solutions were measured at lysozyme concentrations of 20 and 40 mg/mL and precipitant concentrations of 0.4 M at a temperature of 20 °C. The precipitants were inorganic salts: alkaline (NaCl, KCl, and LiCl) and transition-metal (NiCl₂ and CuCl₂) chlorides. Lysozyme solutions without precipitants were measured for comparison. All crystallization conditions were prepared and measured twice.

The energy was 10 keV ($\lambda = 0.124$ nm), and a PILATUS 6M 2D detector was used, which makes it possible to record relatively weak scattering signals. The sample-to-detector distance was 3.0 m, and the SAXS data were recorded in the range of backscattering vectors $s = 0.02$ – 7.0 nm⁻¹, which corresponds to a resolution of 300–0.9 nm in real space. The SAXS measurements were carried out using a specialized cell for the samples, which consists of a horizontal thermostatted (in the range from 278 to 323 K) quartz capillary with 50 μ m thick walls and a diameter of 1.7 mm, enclosed in a special stainless-steel housing. The exposure time was 50 ms (20 scans were made for each sample measurement). The beamline was described in more detail in [11]. The sample volume was 40 μ L in each measurement.

The experimental intensity curves versus the momentum transfer s (where $s = \frac{4\pi \sin \theta}{\lambda}$, 2θ —scattering angle, λ —X-ray wavelength) for protein solutions under different conditions were obtained. The angular range was $0.03 < s < 5.0$ nm⁻¹. When comparing consecutive frames, no radiation damage was detected on the tested samples. The signal averaging from the buffer solution (subtraction of the average signal from the buffer from the experimental protein solution scattering data and normalization for protein concentration) was performed using the program PRIMUS included in the ATSAS software package [12,13].

After the initial treatment, the experimental small-angle scattering curves were processed using the program OLIGOMER [13] to determine the volume fractions of monomers and oligomers of different orders. Calculation of theoretical curves of oligomeric components was carried out using the program CRY SOL [14].

MD simulation. Dimer and octamer models were obtained using the structures of lysozyme tetragonal crystals (HEWL) deposited in the Protein Data Bank (PDB ID: 4WLD and 6QWY) by PyMol software version 1.5 [15]. There were four types of oligomer models characterized by the presence of precipitant ions bound to the protein:

- Without any ions (4WLD);
- Only with cations (one Na⁺ ion per molecule, 4WLD);
- Only with anions (four Cl⁻ ions per molecule, 6QWY);
- With all ions (three Na⁺ and four Cl⁻ ions per molecule, 6QWY).

Protonation states of amino acid residues at pH 4.5 (according to the experimental conditions) were defined using PROPKA server (Version 2.0.0 [16]). All calculations were performed in the Amber ff99SB-ILDN field [17] using GROMACS package version 5.0.4 [18] and TIP4P-Ew water model [19]. The NaCl precipitant concentration in the box was 0.4 M, according to the crystallization conditions.

The energy of each system was minimized using the steepest descent algorithm (50,000 steps) so that the force acting on any atom did not exceed 1000 kJ M⁻¹nm⁻². Then NVT- and NPT- equilibrations were performed by the modified Berendsen (V-rescale) [20] and Parrinello–Rahman methods [21], respectively (for 100 ps each). The integration time step was set at 2 fs, the temperature and pressure were 283 K and 1 atm. Productive MD was calculated in NPT ensemble using modified Berendsen thermostat and Parrinello–Rahman barostat. Integration was carried out by standard leap-frog algorithm [22]. The duration of each trajectory was 100 ns.

3. Results and Discussion

The addition of precipitant to the lysozyme solution leads to a change in the oligomeric composition of the solution, when multimers (higher-order oligomers: dimers, octamers) begin to form along with monomeric particles.

Initial models of oligomers and monomers for processing SAXS data were obtained from two types of structures differing in the number of bound ions: from the lysozyme structure with PDB ID: 4WLD including only one sodium ion, and from structure with PDB IDs: 6QWW, 6QWX, 6QWY, 6QWZ, and 6QX0, for which the positions of chloride ions and additional metal ions bound to the lysozyme molecule were determined in the lattice. In [7], it was determined that under conditions with different precipitants, the number of cations (Cu^{2+} , Ni^{2+} , Na^+ , K^+ , and Li^+) and anions (Cl^-) bound to the lysozyme molecule is different (Figure 1). Note that in view of the low electron density of the Li atom, it was not possible to determine its position, in the case of the KCl precipitant, the K^+ cations associated with the lysozyme molecule were not found, and the largest number of precipitant ions bound to the lysozyme molecule was in copper crystals (four copper ions and six chloride ions).

The calculation of the theoretical scattering curves of oligomeric components was carried out using the program CRY SOL, while a monomeric component was taken from the crystallographic structure of the lysozyme monomer from Protein Data Bank either with ID: 4WLD (Table 1, bold) or with ID: 6QX0, 6QWY, 6QWZ, 6QWX, and 6QWW (Table 1, italics) for each precipitant LiCl, NaCl, KCl, NiCl_2 , and CuCl_2 , respectively. Dimer, tetramer, hexamer, and octamer models were prepared according to the procedure described in [4]. The fit quality of the calculated models to the experimental data obtained in the work [23] was estimated by minimizing the discrepancy χ^2 between the experimental data and the theoretical models according to the formula given in [6]. The radii of gyration and the volume fractions of the oligomeric components in solution with the addition of various precipitants, as determined by SAXS experimental data using the program OLIGOMER (Figure S1), are shown in Table 1.

Table 1. Volume fractions of monomers and oligomers (dimers and octamers) of lysozyme in polydisperse solution with the addition of precipitants LiCl, NaCl, KCl, NiCl_2 , and CuCl_2 (salt concentration 0.4 M) at temperature 20 °C and radii of gyration R_g , obtained from small-angle scattering curves. The results of processing with oligomers based on structures with PDB IDs: 6QX0, 6QWY, 6QWZ, 6QWX, and 6QWW are indicated in italics, with PDB ID: 4WLD—bold. For each precipitant, the data from two independent measurements (1 and 2) are presented. The percentage of tetramers and hexamers is 0% and is not given in the table.

Protein Concentration, mg/mL	Precipitant	Measurement Number	R_g , Å	Monomers, %	Dimers, %	Octamers, %	χ^2
20	-	1	14.37 ± 0.2	100	-	-	3.17
	LiCl	1	<i>19.6 ± 0.2</i>	<i>78.8 ± 0.4</i>	<i>18.8 ± 0.4</i>	<i>2.4 ± 0.1</i>	<i>1.27</i>
			19.7 ± 0.2	80.0 ± 0.4	17.5 ± 0.4	2.5 ± 0.1	1.18
	LiCl	2	<i>19.4 ± 0.2</i>	<i>79.9 ± 0.4</i>	<i>17.8 ± 0.4</i>	<i>2.3 ± 0.1</i>	<i>1.31</i>
			19.5 ± 0.2	81.1 ± 0.4	16.5 ± 0.4	2.4 ± 0.1	1.17
	NaCl	1	<i>18.8 ± 0.2</i>	<i>81.9 ± 0.4</i>	<i>16.2 ± 0.4</i>	<i>1.9 ± 0.1</i>	<i>1.08</i>
			18.9 ± 0.2	83.4 ± 0.4	14.7 ± 0.4	1.9 ± 0.1	1.02
	NaCl	2	<i>19.3 ± 0.2</i>	<i>82.6 ± 0.4</i>	<i>15.0 ± 0.4</i>	<i>2.4 ± 0.1</i>	<i>1.10</i>
			19.4 ± 0.2	84.1 ± 0.4	13.5 ± 0.4	2.4 ± 0.1	1.06
	KCl	1	<i>19.5 ± 0.2</i>	<i>82.6 ± 0.4</i>	<i>14.8 ± 0.4</i>	<i>2.6 ± 0.1</i>	<i>1.06</i>
			19.6 ± 0.2	83.2 ± 0.4	14.3 ± 0.4	2.5 ± 0.1	1.04
	KCl	2	<i>18.8 ± 0.2</i>	<i>84.4 ± 0.4</i>	<i>13.6 ± 0.4</i>	<i>2.0 ± 0.1</i>	<i>1.05</i>
			18.9 ± 0.2	85.0 ± 0.4	13.0 ± 0.4	2.0 ± 0.1	1.04

Table 1. Cont.

Protein Concentration, mg/mL	Precipitant	Measurement Number	R_g , Å	Monomers, %	Dimers, %	Octamers, %	χ^2
40	NiCl ₂	1	<i>19.0 ± 0.2</i>	<i>86.6 ± 0.4</i>	<i>11.1 ± 0.4</i>	<i>2.3 ± 0.1</i>	<i>1.09</i>
			19.2 ± 0.2	89.8 ± 0.4	7.7 ± 0.4	2.5 ± 0.1	1.02
	NiCl ₂	2	<i>19.1 ± 0.2</i>	<i>87.0 ± 0.4</i>	<i>10.5 ± 0.4</i>	<i>2.5 ± 0.1</i>	<i>1.06</i>
			19.3 ± 0.2	90.2 ± 0.4	7.1 ± 0.4	2.7 ± 0.1	1.00
	CuCl ₂	1	<i>18.2 ± 0.2</i>	<i>90.6 ± 0.4</i>	<i>7.7 ± 0.4</i>	<i>1.7 ± 0.1</i>	<i>1.05</i>
			18.1 ± 0.2	88.6 ± 0.4	9.8 ± 0.4	1.6 ± 0.1	1.03
	CuCl ₂	2	<i>18.9 ± 0.2</i>	<i>94.4 ± 0.4</i>	<i>3.2 ± 0.4</i>	<i>2.4 ± 0.1</i>	<i>1.05</i>
			18.8 ± 0.2	92.4 ± 0.4	5.3 ± 0.4	2.3 ± 0.1	1.02
	-	1	14.37 ± 0.2	100	-	-	3.11
	LiCl	1	<i>23.1 ± 0.2</i>	<i>74.9 ± 0.4</i>	<i>18.2 ± 0.4</i>	<i>6.9 ± 0.1</i>	<i>1.91</i>
			23.2 ± 0.2	75.6 ± 0.4	17.6 ± 0.4	6.8 ± 0.1	1.52
	LiCl	2	<i>23.0 ± 0.2</i>	<i>74.8 ± 0.4</i>	<i>18.5 ± 0.4</i>	<i>6.7 ± 0.1</i>	<i>1.83</i>
			23.1 ± 0.2	75.5 ± 0.4	17.9 ± 0.4	6.6 ± 0.1	1.57
	NaCl	1	<i>21.9 ± 0.2</i>	<i>77.5 ± 0.4</i>	<i>17.2 ± 0.4</i>	<i>5.3 ± 0.1</i>	<i>1.49</i>
			22.0 ± 0.2	78.5 ± 0.4	16.4 ± 0.4	5.1 ± 0.1	1.31
	NaCl	2	<i>21.9 ± 0.2</i>	<i>77.8 ± 0.4</i>	<i>16.9 ± 0.4</i>	<i>5.3 ± 0.1</i>	<i>1.55</i>
			22.0 ± 0.2	78.7 ± 0.4	16.1 ± 0.4	5.2 ± 0.1	1.37
	KCl	1	<i>21.7 ± 0.2</i>	<i>80.5 ± 0.4</i>	<i>14.5 ± 0.4</i>	<i>5.0 ± 0.1</i>	<i>1.28</i>
			21.8 ± 0.2	80.8 ± 0.4	14.4 ± 0.4	4.8 ± 0.1	1.23
	KCl	2	<i>21.4 ± 0.2</i>	<i>80.4 ± 0.4</i>	<i>15.0 ± 0.4</i>	<i>4.6 ± 0.1</i>	<i>1.18</i>
21.5 ± 0.2			80.6 ± 0.4	14.9 ± 0.4	4.5 ± 0.1	1.24	
NiCl ₂	1	<i>21.9 ± 0.2</i>	<i>83.7 ± 0.4</i>	<i>11.0 ± 0.4</i>	<i>5.3 ± 0.1</i>	<i>1.22</i>	
		22.1 ± 0.2	86.7 ± 0.4	7.9 ± 0.4	5.4 ± 0.1	1.04	
NiCl ₂	2	<i>21.9 ± 0.2</i>	<i>83.7 ± 0.4</i>	<i>11.0 ± 0.4</i>	<i>5.3 ± 0.1</i>	<i>1.22</i>	
		22.1 ± 0.2	86.7 ± 0.4	7.9 ± 0.4	5.4 ± 0.1	1.04	
CuCl ₂	1	<i>20.9 ± 0.2</i>	<i>92.0 ± 0.4</i>	<i>3.8 ± 0.4</i>	<i>4.2 ± 0.1</i>	<i>1.30</i>	
		20.9 ± 0.2	89.8 ± 0.4	6.1 ± 0.4	4.1 ± 0.1	1.19	
CuCl ₂	2	<i>20.9 ± 0.2</i>	<i>91.5 ± 0.4</i>	<i>4.4 ± 0.4</i>	<i>4.1 ± 0.1</i>	<i>1.21</i>	
		20.9 ± 0.2	89.8 ± 0.4	6.1 ± 0.4	4.1 ± 0.1	1.19	

In general, the results of the modeling obtained using the structure models including all precipitant ions (Table 1, in italics) are similar to the ones for a model with one sodium ion in the structure of the lysozyme molecule (Table 1, on bold). All trends—the absence of tetramers and hexamers, an increase in the number of octamers with an increase in the protein concentration—are consistent with the previously obtained data [4–6,24]. The volume fractions of octamers using two types of models differ by 0.1–0.2%; the volume fractions of dimers—by an average of 1–3%.

However, the fit quality (χ^2) is slightly worsened when using models that take into account all precipitant ions in the structure; small differences between the calculated and experimental curves in the area of wide angles are observed ($s > 0.3 \text{ \AA}^{-1}$). A divergence at this angular range may indicate that not all precipitant ions defined in the crystal structure

are present in the lysozyme oligomer structure in the crystallization solution. Perhaps, some of them are in dynamic equilibrium or dissociate.

Moreover, it is known that protein crystallization mainly depends on the precipitant anions that are chloride ions in the case of lysozyme [1]. Interestingly, the dimer formation with only sodium cation associated with lysozyme is slightly more energetically favorable than it is when all precipitant ions (three sodium and four chlorides) are embedded at NaCl concentrations of 0.4 and 0.6 M [10]. At 0.4 M NaCl in solution, change in free energy upon the binding of lysozyme monomers calculated by MM/GBSA method was -7.87 kcal/M in the case that only Na^+ ions were taken into account, while it was -7.78 kcal/M when Na^+ and Cl^- were incorporated. At 0.6 M NaCl, free energy change was -7.97 and -7.85 kcal/M for cases of only Na^+ and both Na^+ and Cl^- , respectively.

To test this assumption and to find out the impact of precipitant ions in the oligomer structure on the fit quality of the calculated models to the experimental SAXS data, the models with different combinations of the precipitant ions incorporated in lysozyme structure were used in the calculations. The analysis was carried out for the data obtained from crystallization solutions with a CuCl_2 precipitant, due to the maximum presence of precipitant ions (four copper ions and six chloride ions) in the lysozyme structure and due to the higher scattering density of copper atoms compared to alkali metal atoms.

The oligomeric composition was estimated using the lysozyme structures (PDB ID: 6QWW) with the different occupancy of cations (Cu^{2+}) and anions (Cl^-). For automatic comparison of all possible combinations of components, the option “-compar” of the program OLIGOMER was employed [12]. Given the experimental scattering from the mixture and theoretical scattering curves of the components, the program OLIGOMER implements a non-negative linear least-squares algorithm to find the volume fractions of the components minimizing the discrepancy (χ^2).

Based on the structure with PDB ID: 6QWW, sets of form factors (monomer–dimer–octamer) were built, taking into account all precipitant ions (set 1), with only cations (metal ions, set 2), with only anions (chloride ions, set 3), and with the complete absence of precipitant ions in the structure (set 4). The results are shown in Table 2.

Table 2. SAXS fit qualities (χ^2) obtained using the lysozyme oligomeric models with the different occupancy of cations (Cu^{2+}) and anions (Cl^-). For each protein concentration, the data from two independent measurements (1 and 2) are given. The best fit qualities χ^2 are shown in bold. The structures based on PDB ID: 6QWW are used.

Protein Concentration, mg/mL	Measurement Number	χ^2 for the Structures with Cations and Anions (Set1)	χ^2 for the Structures with Cations (Set2)	χ^2 for the Structures with Anions (Set3)	χ^2 for the Structures without Ions (Set4)	χ^2 for the Structures from (Set3 + Set4)
20	1	1.0504	1.0414	1.0397	1.0341	1.0339
	2	1.0489	1.041	1.0389	1.0329	1.0327
40	1	1.3043	1.2653	1.2556	1.2266	1.2254
	2	1.2067	1.1703	1.1596	1.1352	1.1340

In all cases, the best results are obtained by using the combinations consisting of a mixture of set 3 and set 4, that is, the structures without precipitant ions at all and with the occupancy of precipitant anions.

Set 1 is not included in any of the best approximations, which is consistent with the data of Table 1: systematic increase of χ^2 values using models with a full set of cations and anions in the structure as opposed to a model with a single sodium ion. It is worth noting that the program chose oligomers from various sets, practically preserving their ratio from experiment to experiment.

The best approximations are achieved with a set of structures that do not contain precipitant cations at all (monomer, dimer, octamer). The very best approximations consist of a mixture of monomer without ions, as well as dimers and octamers with chlorine ions.

Thus, the occupancy of the protein structures with copper ions and the formation of bonds with the precipitant cation seem to occur after oligomerization and have no significant effect on the formation of precrystallization oligomers, whereas the occupancy of the protein structures with chloride ions and the formation of bonds with the precipitant anion occur already at the early stage of precrystallization.

The stability of oligomers with different occupancy of the protein structures with the precipitant ions (sodium and chlorine) was estimated by root mean square fluctuation (RMSF) from MD simulation. As the molecular dynamics is also sensitive to the “light” and “heavy” for X-ray atoms, the calculations were made for PDB ID: 4WLD and 6QWW.

The higher the RMSF, the less stable the molecule/complex is. Thus, it is obvious from Table 3 that for dimer, the stability decreases while taking into account both cations and anions; only anions; only cations; without ions at all. For octamer, the stability row (from the most to the least) is with cations or anions; without ions at all; with both cations and anions. As the octamer is cluster-precursor for growing crystal, the most probable situation to stabilize oligomers is that with consideration cations or anions in oligomer structure.

Table 3. RMSF of C_{α} atoms of lysozyme dimer and octamer for the cases with the different occupancy of cations (Na^{+}) and anions (Cl^{-}).

Oligomer Type	With Cations and Anions	With Cations	With Anions	Without Ions
Dimer	0.116	0.141	0.130	0.156
Octamer	0.272	0.179	0.182	0.210

In [9], it was shown that it is chlorine ions which stabilize dimer and octamers in crystallization solution. Combining both SAXS and MD results (Figure 2), one can see that the best agreement with experimental SAXS and MD data is reached for oligomers with a minimum number of incorporated chlorine ions.

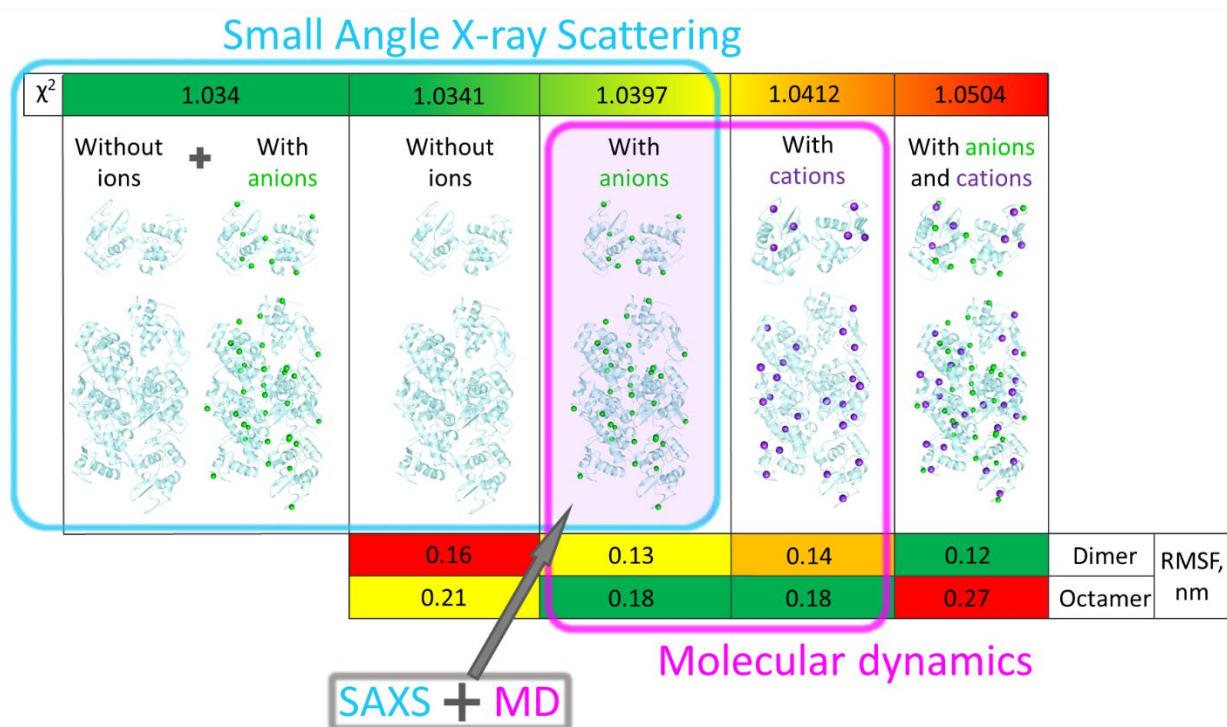


Figure 2. The comparison of results drawn from SAXS and MD data analysis.

It is worthwhile to note that the SAXS data is more sensitive to the atoms with higher electron density (in our case cations), while the molecular dynamics is also sensitive to

the role of anions which are “light” for X-rays. The combination of two methods gives advantages in soft matter’s characterization in comparison to the usage of these methods one by one.

4. Conclusions

The influence of the crystallographic oligomer models with different occupancy of the precipitant ions on the fit quality to the SAXS data was analyzed. Crystallographic structures from Protein Data Bank, 6QWW, 6QWX, 6QWY, 6QWZ, and 6QX0, or 4WLD differing in the number of cations (Cu^{2+} , Ni^{2+} , Na^+ , K^+ and Li^+) and anions (Cl^-) bound to the lysozyme molecule from the maximum presence of precipitant ions (four copper ions and six chloride ions) to the complete absence of precipitant ions in the lysozyme monomer structure, were taken as the monomer components. It has been shown that the best agreement with experimental data is reached for oligomers either without precipitant ions at all or with a minimum number of incorporated chlorine ions. The filling of the protein structures with copper ions and the formation of bonds with the precipitant cation seem to occur after oligomerization and have no significant effect on the formation of pre-crystallization oligomers, opposite to the filling of the protein structures with chloride ions and the formation of bonds with the precipitant anion, according to molecular dynamics [9].

As the SAXS data are more sensitive to the atoms with higher electron density (in our case, cations) and the molecular dynamics is also sensitive to the role of anions which are “light” for X-rays, the combination of these two methods gave the opportunity to define the initial steps before protein crystal growth as the following (Figure 3): firstly, only chloride ions (all found in crystal structure or some of them) associated with monomers and oligomers with these embedded ions are formed, and, finally, cations incorporate in the oligomers, which leads to the formation of crystal, including all precipitant ions bound with it.

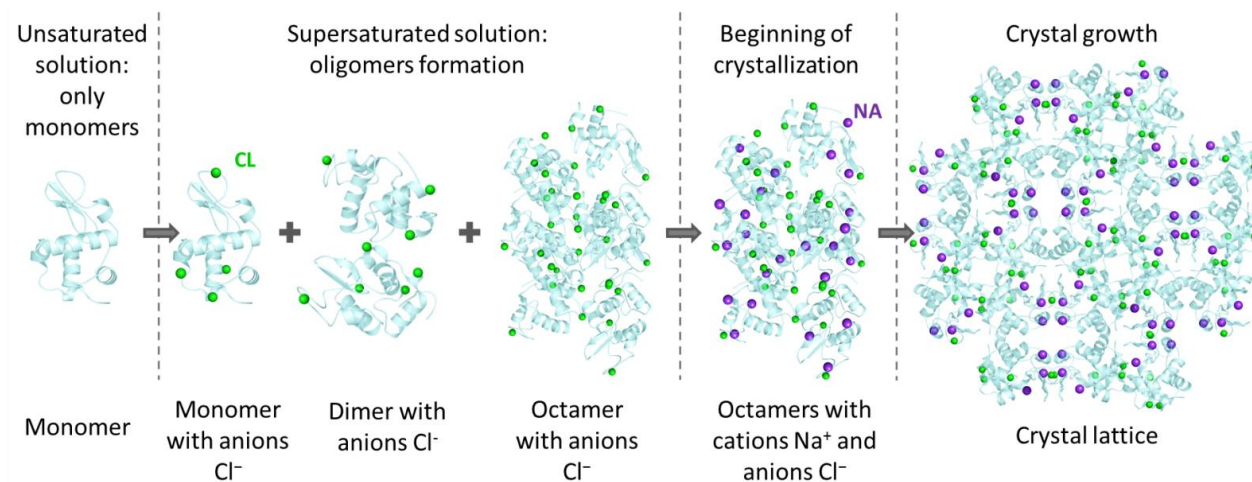


Figure 3. The model of initial steps before protein crystal growth: unsaturated monomer solution → oligomers formation with anions (all found in crystal structure or some of them) association to monomers and oligomers → cations incorporation in the oligomers leading to crystal formation.

Supplementary Materials: The following supporting information can be downloaded at: <https://www.mdpi.com/article/10.3390/cryst12060751/s1>, Figure S1: Experimental SAXS curves (blue curves) for the lysozyme solution with added precipitants (from the top to the bottom) (1) 0.4 M LiCl, (2) 0.4 M KCl, (3) 0.4 M NaCl, (4) 0.4 M NiCl_2 , (5) 0.4 M CuCl_2 and the best OLIGOMER fits (red curves) for the following lysozyme concentrations, respectively: (a) 20 mg/mL (run 1); (b) 20 mg/mL (run 2); (c) 40 mg/mL (run 1); (d) 40 mg/mL (run 2). The curves are shifted along the vertical axis for better visualization.

Author Contributions: Conceptualization, M.A.M.; methodology, P.V.K., M.A.M. and Y.V.P.; software, P.V.K.; validation, Y.V.K. and P.V.K.; formal analysis, Y.V.K. and P.V.K.; physical and computational experiment, Y.V.K., K.B.I., V.I.T., P.V.K. and M.A.M.; resources, A.V.S.; data curation, P.V.K.; original draft preparation, M.A.M. and P.V.K.; writing—review, Y.V.K., P.V.K., M.A.M. and Y.V.P.; editing, M.A.M., P.V.K., Y.V.K., Y.V.P., M.V.K. and A.V.S.; results discussion, M.A.M., P.V.K., Y.V.K., V.I.T., Y.V.P., M.V.K. and A.V.S.; visualization, Y.V.K.; supervision, M.V.K.; project administration, M.A.M.; funding acquisition, A.V.S. All authors have read and agreed to the published version of the manuscript.

Funding: This research was funded by Ministry of Science and Higher Education: grant № 075-15-2021-1363, contract № 208 EI in a part of processing SAXS data and analyzing the results, and the Ministry of Science and Higher Education within the State assignment FSRC «Crystallography and Photonics» RAS in a part of preparing crystallographic models of protein precursor clusters.

Institutional Review Board Statement: Not applicable.

Data Availability Statement: Not applicable.

Acknowledgments: This work has been performed using computing resources of the federal collective usage center Complex for Simulation and Data Processing for Mega-science Facilities at NRC “Kurchatov Institute”, <http://ckp.nrcki.ru/> (accessed on 1 April 2022).

Conflicts of Interest: The authors declare no conflict of interest.

References

1. Ries-Kautt, M.M.; Ducruix, A.F. Relative effectiveness of various ions on the solubility and crystal growth of lysozyme. *J. Biol. Chem.* **1989**, *264*, 745–748. [[CrossRef](#)]
2. Ducruix, A.; Guilloteau, J.P.; Riès-Kautta, M.; Tardieu, A. Protein interactions as seen by solution X-ray scattering prior to crystallogenesis. *J. Cryst. Growth* **1996**, *168*, 28–39. [[CrossRef](#)]
3. Hofmeister, F. Zur Lehre von der Wirkung der Salze. *Arch. Exp. Pathol. Pharmacol* **1888**, *24*, 247–260. [[CrossRef](#)]
4. Kovalchuk, M.V.; Blagov, A.E.; Dyakova, Y.A.; Gruzinov, A.Y.; Marchenkova, M.A.; Peters, G.S.; Pisarevsky, Y.V.; Timofeev, V.I.; Volkov, V.V. Investigation of the Initial Crystallization Stage in Lysozyme Solutions by Small-Angle X-ray Scattering. *Cryst. Growth Des.* **2016**, *16*, 1792–1797. [[CrossRef](#)]
5. Marchenkova, M.A.; Volkov, V.V.; Blagov, A.E.; Dyakova, Y.A.; Ilina, K.B.; Tereschenko, E.Y.; Timofeev, V.I.; Pisarevsky, Y.V.; Kovalchuk, M.V. In situ study of the state of lysozyme molecules at the very early stage of the crystallization process by small-angle X-ray scattering. *Crystallogr. Rep.* **2016**, *61*, 5–10. [[CrossRef](#)]
6. Boikova, A.S.; D'yakova, Y.A.; Il'ina, K.B.; Konarev, P.V.; Kryukova, A.E.; Marchenkova, M.A.; Blagov, A.E.; Pisarevskii, Y.V.; Koval'chuk, M.V. Small-angle X-ray scattering study of the influence of solvent replacement (from H₂O to D₂O) on the initial crystallization stage of tetragonal lysozyme. *Crystallogr. Rep.* **2017**, *62*, 837. [[CrossRef](#)]
7. Marchenkova, M.A.; Kuranova, I.P.; Timofeev, V.I.; Boikova, A.S.; Dorovatovskii, P.V.; Dyakova, Y.A.; Ilina, K.B.; Pisarevskiy, Y.V.; Kovalchuk, M.V. The binding of precipitant ions in the tetragonal crystals of hen egg white lysozyme. *J. Biomol. Struct. Dyn.* **2020**, *38*, 5159–5172. [[CrossRef](#)]
8. Kordonskaya, Y.V.; Timofeev, V.I.; Dyakova, Y.A.; Marchenkova, M.A.; Pisarevsky, Y.V.; Podshivalov, D.D.; Kovalchuk, M.V. Study of the Behavior of Lysozyme Oligomers in Solutions by the Molecular Dynamics Method. *Crystallogr. Rep.* **2018**, *63*, 947–950. [[CrossRef](#)]
9. Kordonskaya, Y.V.; Marchenkova, M.A.; Timofeev, V.I.; Dyakova, Y.A.; Pisarevsky, Y.V.; Kovalchuk, M.V. Precipitant ions influence on lysozyme oligomers stability investigated by molecular dynamics simulation at different temperatures. *J. Biomol. Struct. Dyn.* **2021**, *39*, 7223–7230. [[CrossRef](#)]
10. Kordonskaya, Y.V.; Timofeev, V.I.; Dyakova, Y.A.; Marchenkova, M.A.; Pisarevsky, Y.V.; Kovalchuk, M.V. Free energy change during the formation of crystalline contact between lysozyme monomers under different physical and chemical conditions. *Crystals* **2021**, *11*, 1121. [[CrossRef](#)]
11. Blanchet, C.E.; Spilotros, A.; Schwemmer, F.; Graewert, M.A.; Kikhney, A.; Jeffries, C.M.; Franke, D.; Mark, D.; Zengerle, R.; Cipriani, F.; et al. Versatile sample environments and automation for biological solution X-ray scattering experiments at the P12 beamline (PETRA III, DESY). *J. Appl. Cryst.* **2015**, *48*, 431–443. [[CrossRef](#)] [[PubMed](#)]
12. Franke, D.; Petoukhov, M.V.; Konarev, P.V.; Panjkovich, A.; Tuukkanen, A.; Mertens, H.D.T.; Kikhney, A.G.; Hajjzadeh, N.R.; Franklin, J.M.; Jeffries, C.M.; et al. ATSAS 2.8: A comprehensive data analysis suite for small-angle scattering from macromolecular solutions. *J. Appl. Cryst.* **2017**, *50*, 1212–1225. [[CrossRef](#)] [[PubMed](#)]
13. Konarev, P.V.; Volkov, V.V.; Sokolova, A.V.; Koch, M.H.J.; Svergun, D.I. PRIMUS: A Windows PC-based system for small-angle scattering data analysis. *J. Appl. Crystallogr.* **2003**, *36*, 1277–1282. [[CrossRef](#)]
14. Barberato, C.; Henri, M.; Koch, J.; Svergun, D.; Barberato, C.; Koch, M.H.J. CRY SOL—a program to evaluate X-ray solution scattering of biological macromolecules from atomic coordinates. *J. Appl. Cryst.* **1995**, *28*, 768–773. [[CrossRef](#)]
15. Schrödinger, L.; DeLano, W. PyMOL. 2015. Available online: <http://www.pymol.org/pymol> (accessed on 18 April 2022).

16. Dolinsky, T.J.; Nielsen, J.E.; McCammon, J.A.; Baker, N.A. PDB2PQR: An automated pipeline for the setup of Poisson-Boltzmann electrostatics calculations. *Nucleic Acids Res.* **2004**, *32*, W665–W667. [[CrossRef](#)]
17. Lindorff-Larsen, K.; Piana, S.; Palmo, K.; Maragakis, P.; Klepeis, J.L.; Dror, R.O.; Shaw, D.E. Improved side-chain torsion potentials for the Amber ff99SB protein force field. *Proteins Struct. Funct. Bioinform.* **2010**, *78*, 1950–1958. [[CrossRef](#)] [[PubMed](#)]
18. Van Der Spoel, D.; Lindahl, E.; Hess, B.; Groenhof, G.; Mark, A.E.; Berendsen, H.J.C. GROMACS: Fast, flexible, and free. *J. Comput. Chem.* **2005**, *26*, 1701–1718. [[CrossRef](#)]
19. Horn, H.W.; Swope, W.C.; Pitner, J.W.; Madura, J.D.; Dick, T.J.; Hura, G.L.; Head-Gordon, T. Development of an improved four-site water model for biomolecular simulations: TIP4P-Ew. *J. Chem. Phys.* **2004**, *120*, 9665–9678. [[CrossRef](#)]
20. Berendsen, H.J.C.; Postma, J.P.M.; Van Gunsteren, W.F.; Dinola, A.; Haak, J.R. Molecular dynamics with coupling to an external bath. *J. Chem. Phys.* **1984**, *81*, 3684–3690. [[CrossRef](#)]
21. Parrinello, M.; Rahman, A. Strain fluctuations and elastic constants. *J. Chem. Phys.* **1982**, *76*, 2662–2666. [[CrossRef](#)]
22. Van Gunsteren, W.F.; Berendsen, H.J.C. A Leap-Frog Algorithm for Stochastic Dynamics. *Mol. Simul.* **1988**, *1*, 173–185. [[CrossRef](#)]
23. Marchenkova, M.A.; Konarev, P.V.; Boikova, A.S.; Ilina, K.B.; Pisarevsky, Y.V.; Kovalchuk, M.V. Influence of Chlorides of Mono- and Divalent Metals on the Oligomeric Composition of Lysozyme Crystallization Solutions and Further Crystal Growth. *Crystallogr. Rep.* **2021**, *66*, 751–757. [[CrossRef](#)]
24. Dyakova, Y.A.; Boikova, A.S.; Ilina, K.B.; Konarev, P.V.; Marchenkova, M.A.; Pisarevsky, Y.V.; Timofeev, V.I.; Kovalchuk, M.V. Study of the Influence of a Precipitant Cation on the Formation of Oligomers in Crystallization Solutions of Lysozyme Protein. *Crystallogr. Rep.* **2019**, *64*, 11–15. [[CrossRef](#)]